



Soft Tissue Special Issue: Biphenotypic Sinonasal Sarcoma: A Review with Emphasis on Differential Diagnosis

John Gross¹ · Karen Fritchie¹

Received: 6 September 2019 / Accepted: 26 October 2019 / Published online: 16 January 2020
© Springer Science+Business Media, LLC, part of Springer Nature 2020

Abstract

Biphenotypic sinonasal sarcoma is an anatomically restricted low-grade malignant neoplasm with dual neural and myogenic differentiation composed of a monotonous population of spindled cells with herringbone/fascicular architecture. These tumors demonstrate a unique immunoprofile with relatively consistent S100-protein and actin expression in conjunction with more variable desmin, myogenin and myoD1 staining. SOX10 is uniformly negative. Genetically, the majority of tumors harbor *PAX3-MAML3* fusions, with alternate *PAX3* partners including *FOXO1*, *NCOA1*, *NCOA2* and *WWTR1*. Although the differential diagnosis of BSNS is broad, careful morphologic inspection together with targeted ancillary studies is often sufficient to arrive at the correct diagnosis. As these tumors have significant local recurrence rates but lack metastatic potential, awareness and accurate diagnosis of this rare and newly described neoplasm is critical for appropriate management.

Keywords Sinonasal · Sarcoma · *PAX3* · *MAML3* · Soft tissue

Introduction

Biphenotypic sinonasal sarcoma (BSNS) is a rare locally aggressive site-specific sarcoma that arises in the sinonasal tract and is characterized by *PAX3* rearrangements. First recognized as “low grade sinonasal sarcoma with neural and myogenic differentiation” by Lewis et al., this tumor had undoubtedly been previously misdiagnosed as various benign and malignant mesenchymal neoplasms due to its morphologic and immunophenotypic diversity [1]. As these tumors are low-grade sarcomas with propensity for local recurrence but not distant metastasis, accurate classification is critical for management. This review will highlight the key clinicopathologic features of BSNS with emphasis on its morphologic differential diagnosis to facilitate accurate diagnosis and appropriate treatment.

Clinical Features

A little over one hundred cases of BSNS have been reported in the literature since its initial description less than a decade ago [2–10]. There is a distinct female predominance (female to male ratio of 2:1), and the majority of affected individuals are in the fifth decade of life (age range: 24–87 years; mean 47 years). BSNS typically arises from the upper nasal cavity and ethmoid sinus with fewer cases occurring in the frontal, maxillary and sphenoid sinuses. Intracranial extension or involvement of the orbit or cribriform plate is not uncommon [1, 2]. Consequently, the most common presenting symptoms include nasal congestion or obstruction, epistaxis, pain, sinusitis or purulent rhinorrhea [1, 4]. Magnetic resonance imaging and computed tomography generally show an enhancing soft tissue mass with infiltrative growth associated with hyperostotic bone [11].

Gross and Morphologic Features

Tumor sizes range from 1 to 9 cm (mean approximately 4 cm), and macroscopic examination typically reveals polypoid fragments of firm, reddish-pink to tan-gray tissue [1, 4, 7, 10]. Histologically, BSNS is characterized by an infiltrative proliferation of elongated and monotonous spindle

✉ Karen Fritchie
Fritchie.Karen@mayo.edu

¹ Anatomic Pathology – Department of Laboratory Medicine and Pathology, Mayo Clinic, 200 First Street, SW, Rochester, MN 55905, USA

cells arranged in medium to long fascicles creating a herringbone architecture often with involvement of adjacent bone (Fig. 1a, b). The nuclei may be wavy or focally buckled, reminiscent of the cytologic features of Schwann cells. Although most tumors are predominantly hypercellular, mitotic figures are often difficult to identify (ranging 0–1 mitotic figure/10 high power fields). Only rare cases with increased mitotic activity or focal nuclear pleomorphism have been described, and necrosis is exceedingly rare [4,

7]. Most tumors harbor entrapped invaginations of hyperplastic respiratory epithelium sometimes with squamous metaplasia (Fig. 1c). A minority of cases show areas of rhabdomyoblastic differentiation composed of larger cells with abundant brightly eosinophilic cytoplasm and cross striations (Fig. 1d) [1, 2, 4, 5, 7]. The background stroma often contains foci of prominent vasculature, which may be “hemangiopericytoma-like,” and occasional foci of wispy, delicate collagen (Fig. 1e, f).

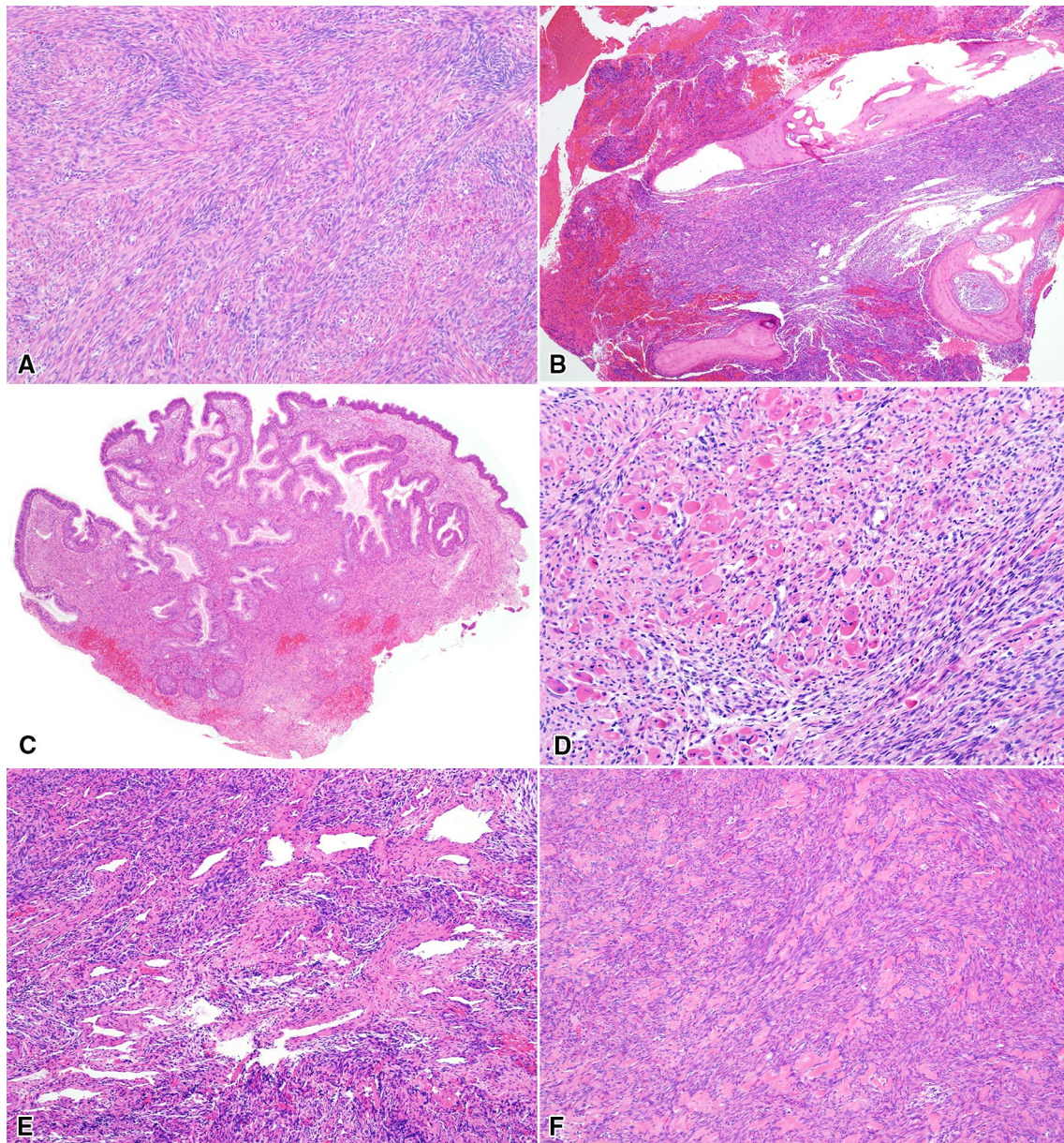


Fig. 1 Histologic examination of biphenotypic sinonasal sarcoma (BSNS) shows a monotonous population of spindle cells with herringbone/fascicular architecture (a). Infiltration into surrounding bone (b) and an associated proliferation of benign respiratory epithelium

(c) are common findings. Rare cases may show rhabdomyoblastic differentiation (d). Other characteristic histologic features of BSNS include branching and hyalinized blood vessels (e) and foci of stromal hyalinization (f)

Immunophenotypic Findings

BSNS expresses a combination of neural and myogenic markers with the vast majority of tumors demonstrating immunoreactivity for both S100 and smooth muscle markers (smooth muscle actin, muscle specific actin or calponin), although the intensity and extent of staining spans from patchy to diffuse (Fig. 2) [1–5, 7, 8, 10]. Other myogenic markers including desmin, myoD1 and myogenin

show patchy to focal staining at best [2–5, 7–10]. Notably, SOX10 is consistently negative [4, 7, 8]. The overwhelming majority of BSNS harbor *PAX3* rearrangements, and recently Jo and colleagues showed that monoclonal *PAX3* is a sensitive and specific marker for this tumor [5]. *PAX8* and polyclonal *PAX3* expression are highly sensitive for BSNS but lack specificity [5, 8]. Variable staining for nuclear beta-catenin may be appreciated in up to approximately 90% of cases with weak to moderate intensity, while both Wang and Jo showed expression of *NTRK3*

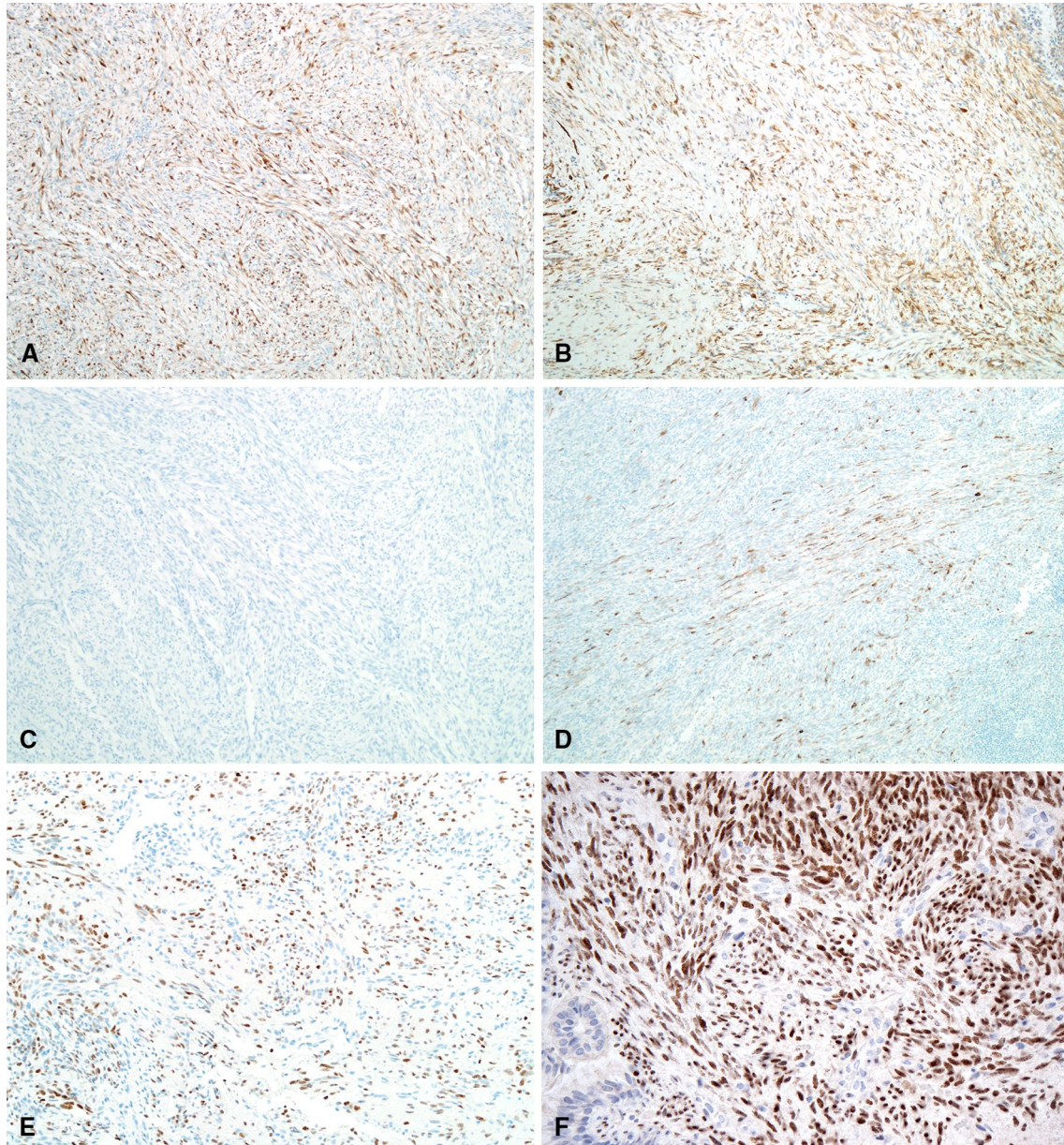


Fig. 2 BSNS shows relatively consistent expression of S100 protein (a) and smooth muscle actin (b), although the intensity of staining is heterogeneous. SOX10 is uniformly negative (c). Patchy to focal immunoreactivity for other myogenic markers including desmin

(d) and myoD1 (e) is common. Monoclonal *PAX3* is also a reliable marker of the diagnosis of BSNS (f) (Photo credit to Dr. Vickie Jo, Brigham and Women's, Boston, MA)

protein and pan-TRK, respectively, in the majority of cases tested [5, 7–9]. H3K27me3 appears to show at least partial staining in BSNS, and focal positivity for other markers such TLE1, cytokeratin, CD34 and EMA may be seen on occasion [1, 5, 7, 10].

Molecular Genetics

Cytogenetic studies performed on two cases in the sentinel series of BSNS by Lewis et al. demonstrated the recurring translocation t(2;4) (q35q31.1). Subsequent work by the same group showed that these tumors harbor a novel *PAX3-MAML3* transcript [1, 9]. While *PAX3-MAML3* represents the most common fusion identified (approximately 60% of cases), alternate *PAX3* partners include *FOXO1*, *NCOA1*, *NCOA2* and most recently *WWTR1* [3, 4, 7, 10]. A small subset of cases appears to harbor isolated *PAX3* or *MAML3* rearrangements or no detectable fusions [3]. The *PAX3-MAML3* fusion protein results in increased activity of *PAX3* response elements, and the presence of alternate fusions involving *FOXO1*, *NCOA1* and *NCOA2* is not surprising given their structural and functional overlap [3, 9]. *PAX3* plays a critical role in neural and skeletal muscle differentiation and development helping to promote lineage commitment and impede terminal differentiation, likely accounting for the dual phenotype of BSNS [12–15]. Additionally, despite the consistent absent of SOX10 staining, gene expression profiles have demonstrated alterations of numerous genes involved in neurogenic development including *NTRK3*, *ALX1-4*, *DBX1*, *GREM1* and *NUROG2*, supporting the tumor's biphenotypic designation [9].

Differential Diagnosis

As BSNS displays both neural and myogenic features, its differential diagnosis includes peripheral nerve sheath tumors as well as neoplasms with skeletal muscle or myoid differentiation (Table 1). Additional considerations include spindle cell mesenchymal neoplasms with oncogenic fusions including solitary fibrous tumor and synovial sarcoma. Since BSNS is anatomically restricted to the sinonasal region, careful morphologic inspection in conjunction with a targeted immunohistochemical work-up usually allows for accurate classification.

One of the primary diagnostic considerations when evaluating a spindle cell neoplasm with some degree of S100 protein expression is a peripheral nerve sheath tumor. Consequently, it is not surprising that a subset of BSNS have likely been erroneously classified as schwannomas or malignant peripheral nerve sheath tumors [1, 16–18]. Both conventional and cellular schwannomas may be differentiated from

BSNS by the presence of circumscribed growth, hyalinized vasculature, and diffuse S100 protein/SOX10 staining, while the former will also display alternating Antoni A/B zones and Verocay bodies (Fig. 3a, b). These features contrast with BSNS which shows infiltrative growth, variable S100 protein expression and lack of SOX10 staining.

High-grade malignant peripheral nerve sheath tumors show some combination of a high mitotic rate, cytologic atypia and necrosis which are features lacking in BSNS (Fig. 3c). Additional clues to the diagnosis of high-grade malignant peripheral nerve sheath tumors include a marbled low power appearance with alternating hyper- and hypocellular zones and increased perivascular cellularity. Low-grade malignant peripheral nerve sheath tumors, on the other hand, show considerable histologic overlap with BSNS (Fig. 3e). Up to 50% of malignant peripheral nerve sheath tumors occur in patients with neurofibromatosis type 1 (NF1), and this clinical feature or identification of a precursor neurofibroma would help support the diagnosis [19]. Histone H3K27 trimethylation (H3K27me3) may be useful in a subset of cases as complete loss is identified in up to approximately 70% of high grade malignant peripheral nerve sheath tumors [20–25]. However, loss of this marker is not entirely specific for malignant peripheral nerve sheath tumors, and its sensitivity in low-grade tumors is significantly lower [21–24, 26, 27]. While limited SOX10 staining would favor malignant peripheral nerve sheath tumor as BSNS should be negative for this marker, S100 protein is of limited utility as focal staining may be seen in both entities (Fig. 3d, f).

Malignant neoplasms with rhabdomyoblastic differentiation are also included in the differential diagnosis. Similar to BSNS, spindle cell rhabdomyosarcoma exhibits herringbone/fascicular architecture, but the mitotic rate and degree of atypia in the latter are usually more significant (Fig. 4a, b). Furthermore, spindle cell rhabdomyosarcoma shows more extensive desmin expression than BSNS, and cases with *MYOD1* mutations show diffuse myoD1 positivity (Fig. 4c, d) [28] [29, 30]. *PAX3* immunohistochemistry may also be helpful in this setting as Jo and colleagues showed that the majority of spindle cell rhabdomyosarcomas are negative for this marker [5]. Heterologous rhabdomyoblastic differentiation may be seen in high-grade malignant peripheral nerve sheath tumors, but, again, these lesions will exhibit significant atypia, frequent mitotic figures and areas of necrosis.

Sinonasal hemangiopericytoma (glomangiopericytoma) is a rare tumor with myoid differentiation composed of bland plump spindled or ovoid-shaped cells arranged in short fascicles or whorls (Fig. 5a, b). Perivascular and stromal hyalinization are common. Given their myoid phenotype, the tumor cells of sinonasal hemangiopericytoma have more abundant pale eosinophilic cytoplasm compared

Table 1 Histologic and immunophenotypic characteristics of biphenotypic sinonasal sarcoma and its mimics

	Histology						Immunohistochemistry				
	Growth pattern	Architecture	Cytology	Mitotic activity	S100 protein	SOX10	Desmin	Myogenin/myoD1			
Biphenotypic sinonasal sarcoma	Infiltrative	Medium to long fascicles/herringbone	Bland spindle cells with scant cytoplasm	0–1/10 HPFs	Patchy to diffuse	Negative	Patchy to focal	Patchy to focal			
Cellular schwannoma	Circumscribed but unencapsulated	Short fascicles or long fascicles/herringbone	Spindle cells with hyperchromatic wavy nuclei	<4/10 HPFs	Diffuse	Diffuse	Negative	Negative			
MPNST, low grade	Fusiform	Long fascicles/herringbone	Spindle cells with hyperchromatic wavy nuclei and atypia	Low	Focal to negative	Focal to negative	Focal to negative	Negative			
MPNST, high grade	Fusiform	Long fascicles/herringbone	Spindle cells with hyperchromatic wavy nuclei and atypia	Brisk	Focal to negative	Focal to negative	Focal to negative	Negative			
MPNST with heterologous rhabdomyoblastic differentiation	Fusiform	Long fascicles/herringbone	Spindle cells with hyperchromatic wavy nuclei and atypia admixed with rhabdomyoblasts	Brisk	Focal to negative	Focal to negative	Focal	Focal			
Spindle cell rhabdomyosarcoma	Typically circumscribed	Long fascicles/herringbone	Spindle cells with scant cytoplasm	High	Negative	Negative	Positive	Focal to diffuse			
Sinonasal hemangiopericytoma	Polypoid and lobulated	Short fascicles or whorls	Oval to spindle cells with pale cytoplasm	Low	Negative	Negative	Negative	Negative			
Synovial sarcoma	Typically circumscribed	Long fascicles/herringbone	Uniform spindle cells with scant cytoplasm	Variable	Focal to negative	Focal to negative	Negative	Negative			
Solitary fibrous tumor	Circumscribed	Haphazard	Ovoid to spindle cells with pale cytoplasm	Variable	Negative	Negative	Negative	Negative			
<i>NTRK</i> -rearranged spindle cell neoplasms	Infiltrative	Typically haphazard; fascicles in high grade tumors	Spindle cells with variable atypia	Variable	Positive	Negative	Negative	Negative			

MPNST malignant peripheral nerve sheath tumor, HPFs high power fields

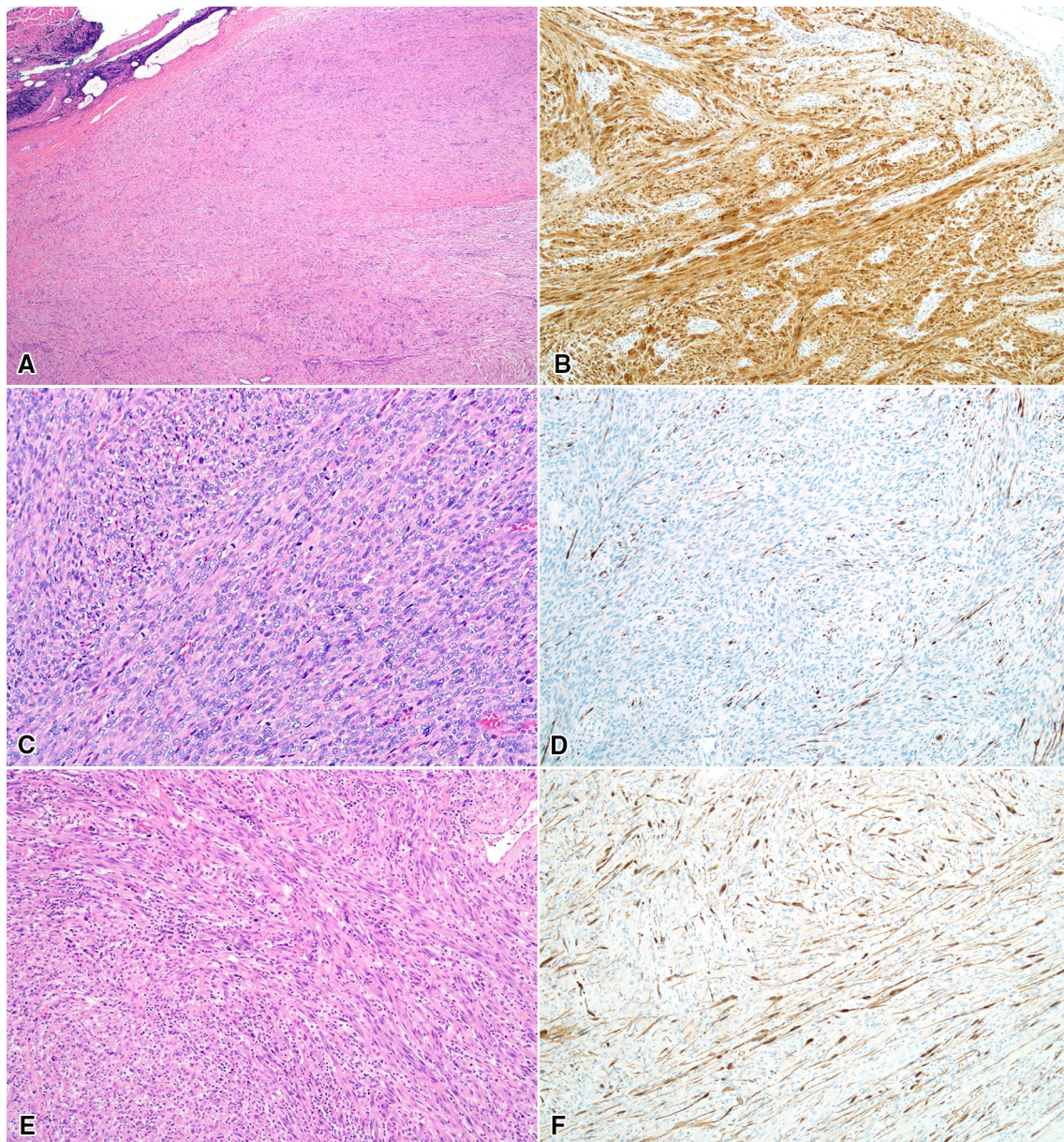


Fig. 3 Cellular schwannomas can often be differentiated from BSNS by their circumscription (a) and strong and diffuse expression of S100 protein (b). High-grade malignant peripheral nerve sheath tumors have more significant cytologic atypia and higher mitotic rates than BSNS (c), although the pattern of S100 protein staining is compar-

able showing only scattered positive tumor cell (d). Low-grade malignant peripheral nerve sheath tumors (e) show considerable morphologic overlap with BSNS in addition to limited positivity for S100 protein (f)

to BSNS and generally show concentric growth around blood vessels. Recent work has shown that *CTNNB1* mutations underlie the tumorigenesis of sinonasal hemangiopericytomas, and, consequently, these tumors are characterized by nuclear β -catenin expression (Fig. 5c) [31, 32]. β -catenin staining is typically focal and less intense in BSNS compared to sinonasal hemangiopericytomas, and sinonasal hemangiopericytomas should not stain for S100, myogenin or myoD1 [8].

As BSNS harbors an oncogenic gene fusion, it has relatively monotonous cytologic features. Consequently, other potential diagnostic mimics include fusion-associated mesenchymal neoplasms with spindled morphology. Monophasic synovial sarcomas, characterized by *SS18-SSX* fusions, exhibit considerable morphologic overlap with BSNS. Both entities are composed of a fascicular or herringbone arrangement of uniform spindled cells with variable stromal hyalinization and a branching vasculature (Fig. 6a). In addition,

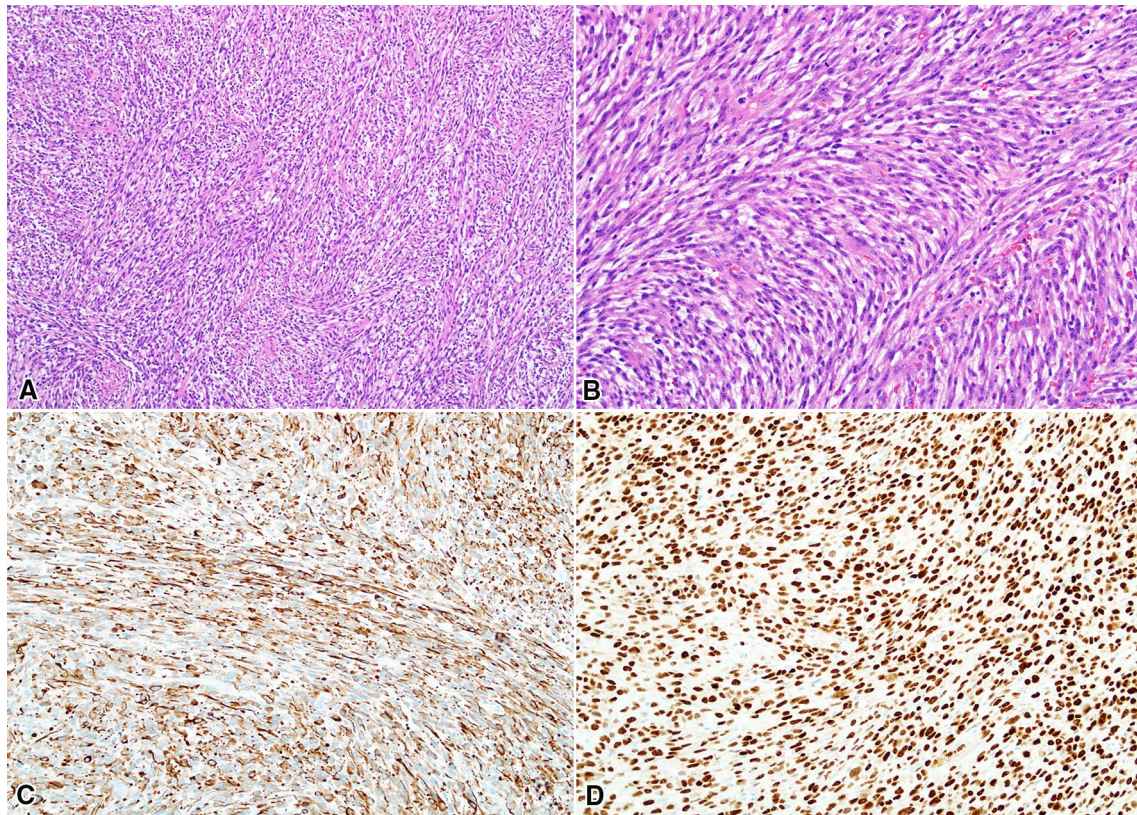


Fig. 4 While spindle cell rhabdomyosarcomas may also harbor a herringbone or fascicular low power architecture (a), close morphologic inspection reveals nuclear hyperchromasia, cytologic atypia

and easily identifiable mitotic figures (b). Additionally, by immunohistochemistry, these tumors show robust staining for desmin (c) and myoD1 (d)

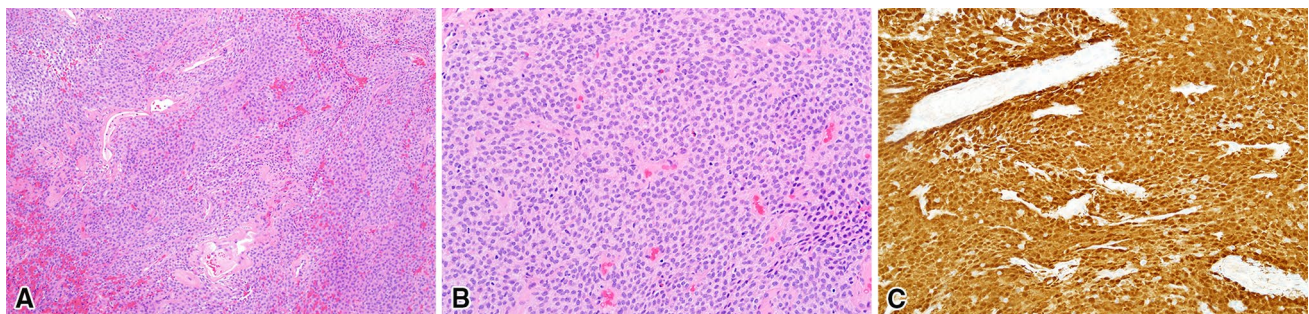


Fig. 5 Sinonasal hemangiopericytoma (glomangiopericytoma) is characterized by plump spindled cells with eosinophilic cytoplasm (a) arranged concentrically around blood vessels (b). Given the pres-

ence of *CTNNB1* mutations, these tumors exhibit strong and diffuse nuclear staining for β -catenin immunostain (c)

immunoreactivity for cytokeratins, EMA, TLE-1 (Fig. 6b) and actins may be seen in both tumors [1, 5, 7, 10]. Expression of desmin, myogenin, myoD1 and PAX3 would favor BSNS, but molecular testing for *SS18* rearrangement may be necessary, especially in small biopsies. Solitary fibrous tumors may occur in the sinonasal region but typically lack the fascicular/herringbone architecture of BSNS, and, instead, show tumor cells with a less organized architecture

(so-called ‘patternless’ pattern) (Fig. 6c). These tumors are characterized by *NAB2-STAT6* fusions, and STAT6 is a highly sensitive and specific marker for this diagnosis (Fig. 6d) [33].

Lewis and colleagues remarked that BSNS closely resembled adult-type fibrosarcoma; however, this diagnosis is now considered one of exclusion due to more extensive immunohistochemical and genetic classification of soft tissue

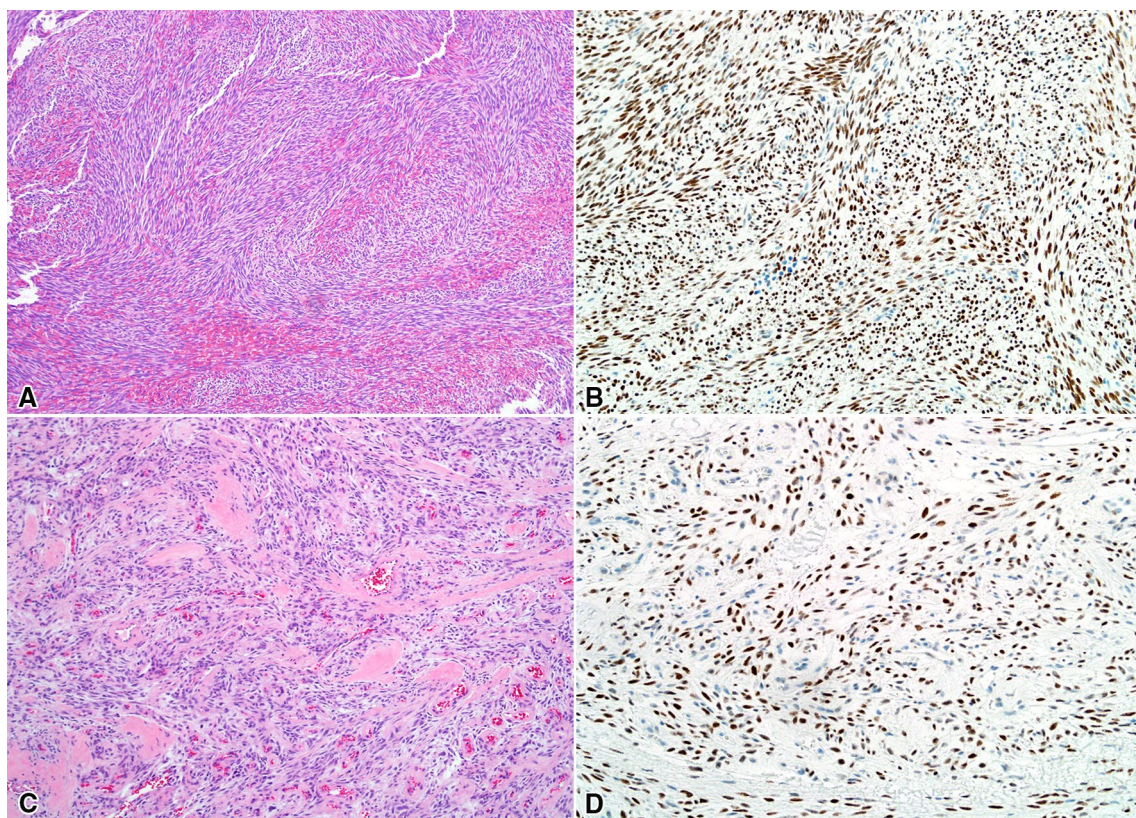


Fig. 6 The low power appearance and cytologic features of BSNS and synovial sarcoma (a) overlaps substantially. Even though synovial sarcoma shows expression of TLE-1 (b), this marker is of limited value in this differential as a subset of BSNS may also stain for this

marker. Unlike BSNS, the tumor cells of solitary fibrous tumor have a disorganized appearance (“patternless pattern”) (c), and STAT6 (d) is a sensitive and specific immunohistochemical stain for this entity

tumors [1]. While adult-type fibrosarcoma may show limited staining for actins, a panel of immunohistochemical stains including S100 protein, SOX10, PAX3 and myogenic markers should allow for differentiation from BSNS.

Finally, a group of *NTRK*-rearranged spindle cell mesenchymal neoplasms with infiltrative growth, areas of prominent keloidal-type stromal hyalinization and co-expression of S100 protein and CD34 has recently emerged (Fig. 7)

[34–36]. Although the morphologic spectrum of these tumors is still evolving, the majority described to date appear to have a haphazard and less organized arrangement of spindle cells, lacking the fascicular/herringbone architecture characteristic of BSNS. While these *NTRK*-fusion neoplasms have features reminiscent of peripheral nerve sheath tumors, similar to BSNS, they lack SOX10 immunoreactivity. Pan-TRK immunostaining appears to be a sensitive

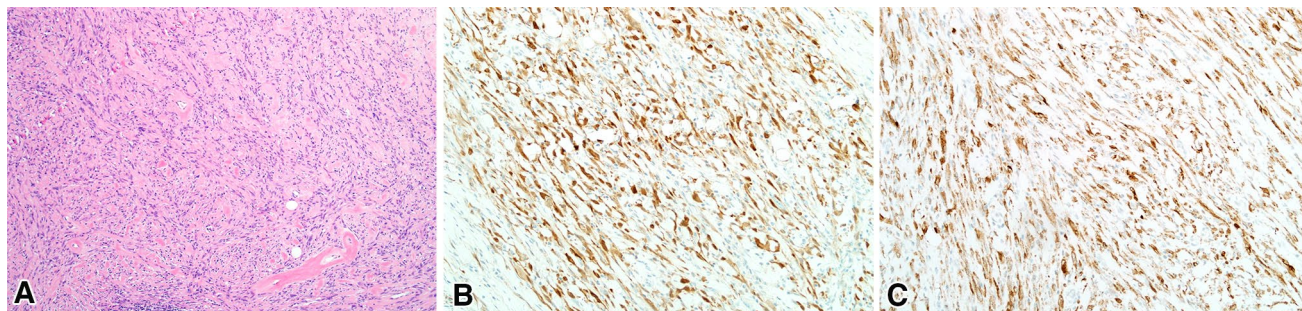


Fig. 7 Mesenchymal neoplasms with *NTRK* rearrangements are composed of relatively uniform spindled cells with variable stromal hyalinization (a). They typically show expression of S100 protein (b) and pan-TRK (c) without SOX10 staining

marker for this group of tumors but is not specific as BSNS may also show pan-TRK expression [5, 37].

Behavior

BSNS is a locally aggressive lesion with propensity for recurrence in approximately 30% of cases, but distant metastases have not been reported to date [2]. Recurrences typically occur within 5 years. There has been a single report of a disease-related death secondary to persistent intracranial growth [8]. Most cases are treated by surgical resection, sometimes requiring orbital exenteration, with or without radiation, and occasional patients may receive adjuvant chemotherapy.

Conclusion

Biphenotypic sinonasal sarcomas are low-grade malignancies harboring *PAX3* rearrangements showing both neural and myogenic features. Consequently, the differential diagnosis of these tumors is broad including peripheral nerve sheath tumors, mesenchymal neoplasms with myoid or rhabdomyoblastic differentiation, and other fusion-associated sarcomas. Awareness of this entity in conjunction with careful morphologic inspection and targeted ancillary work-up should allow for appropriate diagnosis and clinical management.

Compliance with Ethical Standards

Conflict of interest The authors have no conflicts to disclose.

References

- Lewis JT, Oliveira AM, Nascimento AG, et al. Low-grade sinonasal sarcoma with neural and myogenic features: a clinicopathologic analysis of 28 cases. *Am J Surg Pathol*. 2012;36:517–25.
- Andreasen S, Bishop JA, Hellquist H, et al. Biphenotypic sinonasal sarcoma: demographics, clinicopathological characteristics, molecular features, and prognosis of a recently described entity. *Virchows Arch*. 2018;473:615–26.
- Fritchie KJ, Jin L, Wang X, et al. Fusion gene profile of biphenotypic sinonasal sarcoma: an analysis of 44 cases. *Histopathology*. 2016;69:930–6.
- Huang SC, Ghossein RA, Bishop JA, et al. Novel *PAX3-NCOA1* fusions in biphenotypic sinonasal sarcoma With focal rhabdomyoblastic differentiation. *Am J Surg Pathol*. 2016;40:51–9.
- Jo VY, Marino-Enriquez A, Fletcher CDM, et al. Expression of *PAX3* distinguishes biphenotypic sinonasal sarcoma from histologic mimics. *Am J Surg Pathol*. 2018;42:1275–85.
- Kakkar A, Rajeshwari M, Sakthivel P, et al. Biphenotypic sinonasal sarcoma: a series of six cases with evaluation of role of beta-catenin immunohistochemistry in differential diagnosis. *Ann Diagn Pathol*. 2018;33:6–10.
- Le Loarer F, Laffont S, Lesluyes T, et al. Clinicopathologic and molecular features of a series of 41 biphenotypic sinonasal sarcomas expanding their molecular spectrum. *Am J Surg Pathol*. 2019;43:747–54.
- Rooper LM, Huang SC, Antonescu CR, et al. Biphenotypic sinonasal sarcoma: an expanded immunoprofile including consistent nuclear beta-catenin positivity and absence of *SOX10* expression. *Hum Pathol*. 2016;55:44–50.
- Wang X, Bledsoe KL, Graham RP, et al. Recurrent *PAX3-MAML3* fusion in biphenotypic sinonasal sarcoma. *Nat Genet*. 2014;46:666–8.
- Wong WJ, Lauria A, Hornick JL, et al. Alternate *PAX3-FOXO1* oncogenic fusion in biphenotypic sinonasal sarcoma. *Genes Chromosom Cancer*. 2016;55:25–9.
- Cannon RB, Wiggins RH, Witt BL, et al. Imaging and outcomes for a new entity: low-grade sinonasal sarcoma with neural and myogenic features. *J Neurol Surg Rep*. 2017;78:e15–9.
- Wang Q, Fang WH, Krupinski J, et al. Pax genes in embryogenesis and oncogenesis. *J Cell Mol Med*. 2008;12:2281–94.
- Lang D, Lu MM, Huang L, et al. Pax3 functions at a nodal point in melanocyte stem cell differentiation. *Nature*. 2005;433:884–7.
- Medic S, Ziman M. *PAX3* across the spectrum: from melanoblast to melanoma. *Crit Rev Biochem Mol Biol*. 2009;44:85–97.
- Nakazaki H, Reddy AC, Mania-Farnell BL, et al. Key basic helix-loop-helix transcription factor genes *Hes1* and *Ngn2* are regulated by Pax3 during mouse embryonic development. *Dev Biol*. 2008;316:510–23.
- Heffner DK, Gnepp DR. Sinonasal fibrosarcomas, malignant schwannomas, and "Triton" tumors. A clinicopathologic study of 67 cases. *Cancer*. 1992;70:1089–101.
- Hellquist HB, Lundgren J. Neurogenic sarcoma of the sinonasal tract. *J Laryngol Otol*. 1991;105:186–90.
- Gil Z, Fliss DM, Voskoboimik N, et al. Two novel translocations, *t(2;4)(q35;q31)* and *t(X;12)(q22;q24)*, as the only karyotypic abnormalities in a malignant peripheral nerve sheath tumor of the skull base. *Cancer Genet Cytogenet*. 2003;145:139–43.
- Ducatman BS, Scheithauer BW, Piepgras DG, et al. Malignant peripheral nerve sheath tumors. A clinicopathologic study of 120 cases. *Cancer*. 1986;57:2006–21.
- Lee W, Teckie S, Wiesner T, et al. *PRC2* is recurrently inactivated through *EED* or *SUZ12* loss in malignant peripheral nerve sheath tumors. *Nat Genet*. 2014;46:1227–32.
- Rohrich M, Koelsche C, Schrimpf D, et al. Methylation-based classification of benign and malignant peripheral nerve sheath tumors. *Acta Neuropathol*. 2016;131:877–87.
- Schaefer IM, Fletcher CD, Hornick JL. Loss of H3K27 trimethylation distinguishes malignant peripheral nerve sheath tumors from histologic mimics. *Mod Pathol*. 2016;29:4–13.
- Cleven AH, Sanna GA, Briaire-de Bruijn I, et al. Loss of H3K27 tri-methylation is a diagnostic marker for malignant peripheral nerve sheath tumors and an indicator for an inferior survival. *Mod Pathol*. 2016;29:582–90.
- Le Guellec S, Macagno N, Velasco V, et al. Loss of H3K27 trimethylation is not suitable for distinguishing malignant peripheral nerve sheath tumor from melanoma: a study of 387 cases including mimicking lesions. *Mod Pathol*. 2017;30:1677–87.
- Pekmezci M, Cuevas-Ocampo AK, Perry A, et al. Significance of H3K27me3 loss in the diagnosis of malignant peripheral nerve sheath tumors. *Mod Pathol*. 2017;30:1710–9.
- Asano N, Yoshida A, Ichikawa H, et al. Immunohistochemistry for trimethylated H3K27 in the diagnosis of malignant peripheral nerve sheath tumours. *Histopathology*. 2017;70:385–93.
- Prieto-Granada CN, Wiesner T, Messina JL, et al. Loss of H3K27me3 expression is a highly sensitive marker for

- sporadic and radiation-induced MPNST. *Am J Surg Pathol*. 2016;40:479–89.
28. Agaram NP, LaQuaglia MP, Alaggio R, et al. MYOD1-mutant spindle cell and sclerosing rhabdomyosarcoma: an aggressive subtype irrespective of age. A reappraisal for molecular classification and risk stratification. *Mod Pathol*. 2019;32:27–36.
 29. Cavazzana AO, Schmidt D, Ninfo V, et al. Spindle cell rhabdomyosarcoma. A prognostically favorable variant of rhabdomyosarcoma. *Am J Surg Pathol*. 1992;16:229–35.
 30. Carter CS, East EG, McHugh JB. Biphenotypic sinonasal sarcoma: a review and update. *Arch Pathol Lab Med*. 2018;142:1196–201.
 31. Lasota J, Felisiak-Golabek A, Aly FZ, et al. Nuclear expression and gain-of-function beta-catenin mutation in glomangiopericytoma (sinonasal-type hemangiopericytoma): insight into pathogenesis and a diagnostic marker. *Mod Pathol*. 2015;28:715–20.
 32. Haller F, Bieg M, Moskalev EA, et al. Recurrent mutations within the amino-terminal region of beta-catenin are probable key molecular driver events in sinonasal hemangiopericytoma. *Am J Pathol*. 2015;185:563–71.
 33. Doyle LA, Vivero M, Fletcher CD, et al. Nuclear expression of STAT6 distinguishes solitary fibrous tumor from histologic mimics. *Mod Pathol*. 2014;27:390–5.
 34. Agaram NP, Zhang L, Sung YS, et al. Recurrent NTRK1 gene fusions define a novel subset of locally aggressive lipofibromatosis-like neural tumors. *Am J Surg Pathol*. 2016;40:1407–16.
 35. Suurmeijer AJH, Dickson BC, Swanson D, et al. A novel group of spindle cell tumors defined by S100 and CD34 co-expression shows recurrent fusions involving RAF1, BRAF, and NTRK1/2 genes. *Genes Chromosom Cancer*. 2018;57:611–21.
 36. Davis JL, Lockwood CM, Stohr B, et al. Expanding the spectrum of pediatric NTRK-rearranged mesenchymal tumors. *Am J Surg Pathol*. 2019;43:435–45.
 37. Hung YP, Fletcher CDM, Hornick JL. Evaluation of pan-TRK immunohistochemistry in infantile fibrosarcoma, lipofibromatosis-like neural tumour and histological mimics. *Histopathology*. 2018;73:634–44.

Publisher's Note Springer Nature remains neutral with regard to jurisdictional claims in published maps and institutional affiliations.